



# High temporal resolution Br<sub>2</sub>, BrCl and BrO observations in coastal Antarctica

Z. Buys<sup>1,2</sup>, N. Brough<sup>1</sup>, L. G. Huey<sup>3</sup>, D. J. Tanner<sup>3</sup>, R. von Glasow<sup>2</sup>, and A. E. Jones<sup>1</sup>

<sup>1</sup>British Antarctic Survey, NERC, High Cross, Madingley Road, Cambridge, UK

<sup>2</sup>University of East Anglia, School of Environmental Sciences, Norwich, UK

<sup>3</sup>Georgia Institute of Technology, School of Earth and Atmospheric Sciences, Atlanta, USA

Correspondence to: Z. Buys (zakysa@bas.ac.uk)

Received: 23 March 2012 – Published in Atmos. Chem. Phys. Discuss.: 27 April 2012

Revised: 15 January 2013 – Accepted: 23 January 2013 – Published: 1 February 2013

**Abstract.** There are few observations of speciated inorganic bromine in polar regions against which to test current theory. Here we report the first high temporal resolution measurements of Br<sub>2</sub>, BrCl and BrO in coastal Antarctica, made at Halley during spring 2007 using a Chemical Ionisation Mass Spectrometer (CIMS). We find indications for an artefact in daytime BrCl measurements arising from conversion of HOBr, similar to that already identified for observations of Br<sub>2</sub> made using a similar CIMS method. Using the MIS-TRA model, we estimate that the artefact represents a conversion of HOBr to Br<sub>2</sub> of the order of several tens of percent, while that for HOBr to BrCl is less but non-negligible. If the artefact is indeed due to HOBr conversion, then nighttime observations were unaffected. It also appears that all daytime BrO observations were artefact-free. Mixing ratios of BrO, Br<sub>2</sub> and BrCl ranged from instrumental detection limits to 13 pptv (daytime), 45 pptv (nighttime), and 6 pptv (nighttime), respectively. We see considerable variability in the Br<sub>2</sub> and BrCl observations over the measurement period which is strongly linked to the prevailing meteorology, and thus air mass origin. Higher mixing ratios of these species were generally observed when air had passed over the sea-ice zone prior to arrival at Halley, than from over the continent. Variation in the diurnal structure of BrO is linked to previous model work where differences in the photolysis spectra of Br<sub>2</sub> and O<sub>3</sub> is suggested to lead to a BrO maximum at sunrise and sunset, rather than a noon-time maxima. This suite of Antarctic data provides the first analogue to similar measurements made in the Arctic, and of note is that our maximum measured BrCl (nighttime) is less than half of the maximum measured during a similar period (spring-time) in the Arctic

(also nighttime). This difference in maximum measured BrCl may also be the cause of a difference in the Br<sub>2</sub> : BrCl ratio between the Arctic and Antarctic. An unusual event of trans-continental air mass transport appears to have been responsible for severe surface ozone depletion observed at Halley over a 2-day period. The halogen source region appears to be the Bellingshausen Sea, to the west of the Antarctic Peninsula, with the air mass having spent 3 1/2 days in complete darkness crossing the continent prior to arrival at Halley.

## 1 Introduction

The first published measurements of tropospheric ozone depletion events (ODEs) were reported from Barrow, Alaska (Oltmans, 1981), followed by a more detailed study in March 1985 at Alert, Nunavut (Bottenheim et al., 1986). A study by Barrie et al. (1988) was the first to link these ODEs to bromine. Since the first observations of boundary layer (BL) ODEs in the Antarctic in the mid-1990s (Kreher et al., 1996; Wessel et al., 1998) and the coincident detection of BrO (Kreher et al., 1997), many more Antarctic field studies have taken place (Rankin et al., 2002; Jones et al., 2006). Roscoe and Roscoe (2006) showed, through analysis of historical ozone data from Halley, that ozone depletion events were evident as far back as 1957/58.

During ozone depletion events, ozone mixing ratios can fall from background amounts (typically 30–40 ppbv) to below instrumental detection limits (roughly a few parts per billion by volume, ppbv) within a few minutes and remain suppressed for on the order of hours to days.

The chemical destruction of ozone is driven by halogens, especially bromine radicals (e.g. Simpson et al., 2007; Abbatt et al., 2012), the critical reaction being:



Catalytic destruction of ozone is achieved if the bromine radicals are re-generated without production of ozone. This can occur in a number of ways, such as:

(a) via the BrO self-reaction:



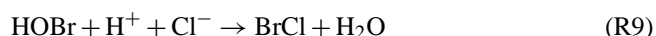
(b) via reaction with HO<sub>2</sub>:



(c) via interhalogen reactions, such as:



There is still much debate over the precise source of atmospheric bromine that drives ODEs, but there is strong observational evidence to suggest a source associated with the sea ice zone (Gilman et al., 2010; Jacobi et al., 2010; Abbatt et al., 2012). Such a source would be consistent with laboratory studies, where heterogeneous reactions have been shown to generate Br<sub>2</sub> and BrCl, via uptake of HOBr onto frozen and dry NaCl/NaBr coated surfaces (Adams et al., 2002; Fickert et al., 1999), via the following multiphase reactions:



Although our knowledge of ODEs and associated chemistry has increased greatly since their discovery, some of the key processes involved are not yet fully understood (Simpson et al., 2007), and high temporal resolution observations of inorganic bromine compounds against which to test current theory are sparse. In 2007, year round measurements were made at the British Antarctic Survey station Halley (75°35' S, 26°19' W), in coastal Antarctica, using a Chemical Ionisation Mass Spectrometer (CIMS). During the austral spring and summer, the CIMS was configured to perform high resolution measurements of BrO, Br<sub>2</sub> and BrCl. In addition, concurrent measurements of surface ozone and local

meteorology were made. Although such observations have been made in the Arctic (Neuman et al., 2010; Liao et al., 2011a, b, 2012b), this is the first such suite of measurements made in Antarctica.

Here we present an analysis of the springtime data. However, we first explore the issue of an apparent CIMS inlet artefact (Neuman et al., 2010) that arises from conversion of HOBr on surfaces, and appears, in our data, to affect both Br<sub>2</sub> and BrCl observations (although not BrO) during sunlit hours. We use the MISTRA model to make an estimate of the influence of this artefact on Br<sub>2</sub> and BrCl, and restrict subsequent discussions of Br<sub>2</sub> and BrCl to nighttime data only. We discuss BrO observations in terms of changes in the diurnal shape throughout the measurement period, and the chemistry responsible for these changes. We, further, explore the influence of air masses passing over different source regions prior to arrival at Halley. As these are the first suite of Antarctic data to provide an analogue to similar measurements made in the Arctic, we compare our observations in the south with those in the north, including differences in the Br<sub>2</sub> : BrCl ratio. Finally we present an unusual event of air mass transport, where the halogen source region associated with severe ozone depletion and the highest measured Br<sub>2</sub> mixing ratio, appears to be to the west of the Antarctic Peninsula.

## 2 Experimental methods

### 2.1 Halley research station

Measurements were made at Halley, an Antarctic coastal research station operated by the British Antarctic Survey (BAS) and situated on the Brunt Ice Shelf, 35 m above sea level. Halley is effectively located on a promontory that extends out into the Weddell Sea and of note, to the south and west is a large area of open water with associated newly-forming sea ice (referred to as Precious Bay). Although the prevailing wind direction at Halley throughout the year is easterly, traversing hundreds of kilometres of undisturbed snow, strong directional changes to westerlies/south-westerlies often occur, especially in the spring and summer months. This results in air masses with very different histories arriving at Halley.

The instruments used for this field campaign were housed in the CASLab (Clean Air Sector Laboratory) which is situated about 1 km south of the main base in an area that is exposed to minimal disturbance by vehicles or base pollution (Jones et al., 2008).

The measurement campaign ran between January 2007 and February 2008. During the year, the CIMS operated alternately in two different modes; (i) a high pressure mode which measured, separately, OH and (HO<sub>2</sub> + RO<sub>2</sub>) and (ii) a low pressure mode measuring a variety of trace gases including HNO<sub>4</sub>, HCl, HNO<sub>3</sub>, SO<sub>2</sub>. In early spring, BrO, BrCl and Br<sub>2</sub> were added to the suite of low pressure measurements

and included over the subsequent low-pressure mode measurement periods. The first direct sunlight at Halley at the end of the polar winter occurs on 13 August, thus the observations reported here almost all fall within the sunlit spring time.

## 2.2 CIMS instrument description

The CIMS technique has been used to detect many atmospheric trace gases (Huey et al., 1995, 1998; Berresheim et al., 2000; Leibrock and Huey, 2000; Huey et al., 2004; Sjostedt and Abbatt, 2008), but its use as a high mass and temporal-resolution halogen detector is of most importance to this present study. While the CIMS technique is well documented (e.g. Huey et al., 2004; Slusher et al., 2004; Liao et al., 2011b), we describe here features that were specific to the configuration at Halley.

Within the CIMS ionisation region, a mixture of nitrogen doped with a few parts per million by volume (ppmv) of SF<sub>6</sub> was added to the flow tube after passing through a <sup>210</sup>Po ion source. This synthesised the reagent ion SF<sub>6</sub><sup>-</sup> in the ion source via associative electron attachment (Huey et al., 2004). The use of SF<sub>6</sub><sup>-</sup> as a reagent ion can be limited due to its slow second-order reaction with water (Huey et al., 1995; Arnold and Viggiano, 2001), but Slusher et al. (2001) have found that it is viable at dew points below ~ -20 °C, such as are frequently found in polar regions.

Ambient air was continually sampled at a high flow rate (~ 2400 slpm) by means of a regenerative blower (Ametek BCDC) into a 40 cm long aluminium pipe of 8 cm inner diameter (i.d.) that protruded 20 cm above the laboratory roof which is roughly 5 m above the snowpack. A smoothed Teflon doughnut-shaped cap was secured to the pipe and positioned in the NE corner of the laboratory which allowed the least perturbed flow thereby minimising turbulence as well as shading.

To further reduce problems associated with surface adsorption, air was sampled from the centre of the aluminium pipe at a flowrate ~ 8 slpm which reduced both the residence and possible wall interaction time ( $t < 0.6$  s). The sampled air was delivered to the CIMS in a heated teflon perfluoroalkoxyalkane (PFA) inlet (i.d. = 0.65 cm, length = 25 cm) controlled at 40 ± 2 °C by a series of thin Kapton heaters. From there, sampled air mixed with ions from the ion source where reactions can occur for the length of the flow tube. A small amount of air from the flow tube is sampled and then electrostatically accelerated by ion optics into the quadrupole mass filter and an ion detector which can detect multiple ion masses on each pass (Huey et al., 2004). Rate coefficients for the reactions of the molecules with SF<sub>6</sub><sup>-</sup> were measured relative to SO<sub>2</sub>, as the rate coefficient for Reaction (R10) has been measured over a wide range of pressures and buffer gases (Slusher et al., 2001). SO<sub>2</sub> is also used as the calibration gas for the instrument.



An automated 3-way sampling valve enabled switching between two flow paths, measurement mode and zero mode, without disrupting the required constant flow (maintained by the diaphragm pump). Background or zero measurements were obtained every 10 min by drawing air through a 20 cm × 5 cm i.d. stainless steel filter tube for a 3 min period. The filter tube contained activated coarse charcoal and nylon glass wool that had been previously soaked and dried in a concentrated NaHCO<sub>3</sub> solution. A similar scrubbing method had previously been successfully employed (Slusher et al., 2004; Liao et al., 2011a).

To determine the sensitivity of the CIMS instrument in the field, a mass flow controller (MKS 1479A) provided a continuous 8 sccm (standard cubic centimeters per minute) flow of 0.2 % (±5σ) of a certified standard of our calibration gas (SO<sub>2</sub> in nitrogen) (Air Products, speciality gases) to the insulated inlet system every two hours for a 1 min period.

As SO<sub>2</sub> was used as our primary calibration gas for the CIMS instrument in the field, we were able to use the sensitivity ratio of SO<sub>2</sub> to Br<sub>2</sub> (determined in the lab after the fieldwork as a function of dew point temperature) as a proxy to track the sensitivity of Br<sub>2</sub>. The ratio of the rate constants for reaction SO<sub>2</sub> + SF<sub>6</sub><sup>-</sup> → F<sub>2</sub>SO<sub>2</sub><sup>-</sup> + SF<sub>4</sub> and Br<sub>2</sub> + SF<sub>6</sub><sup>-</sup> → Br<sub>2</sub><sup>-</sup> + SF<sub>6</sub> could then be used to calibrate the Br<sub>2</sub> measurements after the campaign.

BrO calibration was achieved using a similar method to that described in Sect. 2.2 in Liao et al. (2011a). We use the ratio of the rate constant for the reaction Br<sub>2</sub> + SF<sub>6</sub><sup>-</sup> → Br<sub>2</sub><sup>-</sup> + SF<sub>6</sub> to the reaction BrO + SF<sub>6</sub><sup>-</sup> → BrO<sup>-</sup> + SF<sub>6</sub> (determined to be 1.0 ± 25 % in the laboratory by Liao et al., 2011a), along with the dew point calculation, to determine the BrO calibration.

The measurements were all corrected for humidity (to account for any influence of the slow second-order reaction of SF<sub>6</sub><sup>-</sup> with H<sub>2</sub>O) and converted to mixing ratios.

Limits of detection (LOD) were estimated using 1σ counting precision of the 10 s zero background signal. This approach was used (Ridley et al., 1994) as there was no suitable invariant ambient data. The standard deviation of the zero data was transformed to pptv using the averaged sensitivity of the instrument to SO<sub>2</sub>.

Table 1 gives details of instrument performance, and associated uncertainties in the halogen measurements. The estimated accuracies were obtained from the uncertainties in the flow meter calibrations for the sample and calibration gas obtained with a bubble flow meter before and after each measurement period and was found to be ~ 4 %. This also includes the uncertainty in the calibration gas standard which the manufacturer provided (5σ). The precision of the instrument to SO<sub>2</sub> was obtained from the scatter (1σ) of the SO<sub>2</sub> sensitivity and found to be < 2 % (at a dew point of -24 °C).

**Table 1.** Instrument parameters and overview of observations for BrO, Br<sub>2</sub> and BrCl for the period 12 August–18 September 2007. Details of measurements (max, mean, and standard deviation) for Br<sub>2</sub> and BrCl are based on nighttime observations only – see Sect. 3.2. Minimum values were below detection limits for all three species.

	BrO	Br <sub>2</sub>	BrCl
Sensitivity Hz pptv <sup>-1</sup>	4.9	4.9	4.9
2σ detection limit for 10 min averages (pptv)	0.6	0.4	0.1
Maximum observed (pptv)	13.3 (Day)	45 (Night)	5.9 (Night)
Mean nighttime observation (pptv)	–	5.8	1
Standard deviation of 10 min average (pptv)	2.2	6	1
Measurement uncertainties	±27 %	±11 %	±11 %

### 2.3 Supporting observations

Surface ozone was measured at the CASLab, using a UV absorption technique (Wilson and Birks, 2006). The instrument used was a Thermo Electron model 49C, which has a detection limit of 1 ppbv, and a precision of 1 ppbv. Data were recorded as 1 min averages of 10 s observations. Measurements of wind speed and wind direction were carried out at the main station, some 1 km from the CASLab. The anemometers and vanes were located at a height roughly 10 m above the snow surface, and have an accuracy of about 0.5 m s<sup>-1</sup> for wind speed and 5° for wind direction (König-Langlo et al., 1998). Data are also output every 1 min. Information on sea ice concentration was obtained from the satellite-borne AMSR-E instrument (Sprenn et al., 2008) which provides information at a resolution of 6.25 by 6.25 km.

### 2.4 MISTRA, model description

To explore features in the CIMS observations, we use both the 0-D (box-model) and 1-D versions of the Marine Boundary Layer (MBL) chemistry model, MISTRA (von Glasow et al., 2002).

MISTRA includes descriptions of meteorology, microphysics and thermodynamics as well as a multiphase chemistry module (von Glasow et al., 2002). The chemistry module includes chemical reactions in the gas phase, in and on aerosol particles and takes into account transfer between the gas and aqueous phase. The complete set of chemical reactions incorporated in the multi-phase chemistry module are solved using the kinetic pre-processor (KPP) (Damian

et al., 2002) which allows easy changes of the chemical mechanism.

The model atmosphere in MISTRA 1-D is divided into 150 layers, with the lowest 100 having a constant grid height which can be set in the model (here chosen to be  $\Delta z = 3$  m), and those layers above 100 being spaced logarithmically. Whereas gas phase chemistry is considered in all model layers, aerosol chemistry is only taken into account in layers where the relative humidity is greater than the crystallisation humidity. Dry deposition of gases onto the sea and snow surface is calculated using the resistance model described by Wesely (1989), and photolysis rates are calculated online by the method of Landgraf and Crutzen (1998).

For our work, we initialised the MISTRA model runs using measurements made at Halley station, including: aerosol size distribution and composition (Rankin and Wolff, 2003), local meteorology (Anderson and Neff, 2008), and measurements of local chemical composition (NO<sub>x</sub>, O<sub>3</sub>, NMHCs, DMS, HCHO, CO). All emissions from particles and the surface (lowest model layer) result from explicit condensed-phase chemistry, apart from a prescribed flux of Br<sub>2</sub> from the model surface.

### 2.5 Air mass history

Back trajectory analyses using the Hybrid Single-Particle Lagrangian Integrated Trajectory (HYSPLIT) model were used to track air mass origins. HYSPLIT is available via the NOAA ARL READY website ([www.arl.noaa.gov/ready.php](http://www.arl.noaa.gov/ready.php)) (Rolph, 2012; Draxler and Rolph, 2012). Back trajectories were driven by meteorological fields from the NCEP Global Data Assimilation System (GDAS) model output, and calculated using model vertical velocity at a resolution of 1° by 1°.

## 3 Results and discussion

### 3.1 Investigation of potential interferer in daytime CIMS Br<sub>2</sub> and BrCl observations

A surprising feature in the CIMS halogen data from Halley were the above detection limit observations of both Br<sub>2</sub> and BrCl during daytime (e.g. Fig. 1). If real, the data would suggest either an extremely high flux of bromine radicals into the polar boundary layer, or previously-unknown chemistry. The alternative, however, is that the data are affected by an artefact caused by the sampling methodology.

It has recently been demonstrated that CIMS observations of Br<sub>2</sub> can suffer from an artefact, most likely arising from chemical conversion on the instrument inlet (Neuman et al., 2010). The authors reported HOBr conversion to Br<sub>2</sub> on a number of different surfaces, both coated with NaBr and uncoated, the latter including the Teflon of the instrument inlet, glass, aluminium, stainless steel, PVDF (Polyvinylidene difluoride; a highly non-reactive and pure thermoplastic

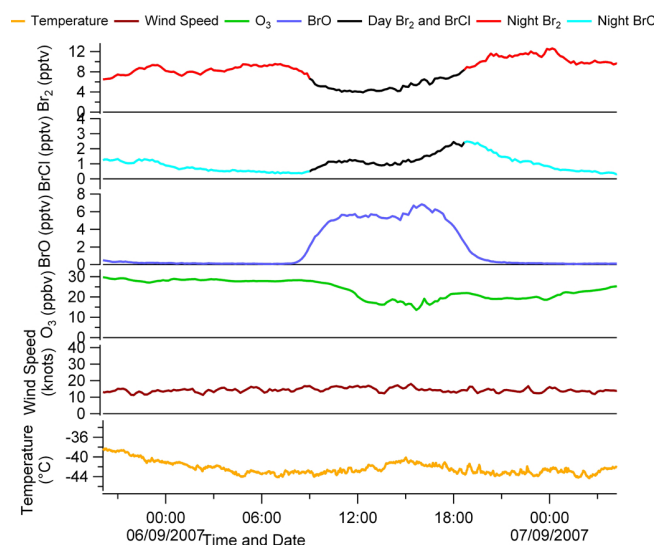


**Fig. 1.** Wind speed, temperature, surface O<sub>3</sub>, and CIMS Br<sub>2</sub>, BrCl and BrO measurements from Halley on 6–7 September 2007. Br<sub>2</sub> and BrCl daytime measurements are coloured black.

fluoropolymer), and several other types of Teflon. Their results are in line with laboratory studies that have shown the rapid generation of Br<sub>2</sub>, and to a lesser extent BrCl, on salty surfaces, via uptake of HOBr (Abbatt, 1994; Adams et al., 2002; Kirchner et al., 1997). The presence of a CIMS inlet artefact in Br<sub>2</sub> has been acknowledged in subsequent field measurements (e.g. Liao et al., 2012a, b).

Before we discuss the data further, we will explore these hypotheses.

To explore the possible presence of a CIMS inlet artefact in our data, we focus on a few days in September during which meteorological conditions were roughly constant (Fig. 1). The local wind direction throughout this period ( $\sim 250^\circ$ ) indicates arrival of air at Halley from over Precious Bay, and wind speeds were constant at  $\sim 7 \text{ m s}^{-1}$ . Temperatures were very low at  $-40^\circ\text{C}$  and observations from an acoustic sounder (a “sodar”), which provides information on atmospheric structure, suggest that there was a well-defined boundary layer (BL) (at  $\sim 200 \text{ m}$  on 6 September). Observations of temperature and horizontal wind speed from an adjacent 30 m mast (sensors at 1, 2, 4, 8, 16, and 32 m) suggest the BL was well mixed on this day. While a box model can be appropriate to study a well-mixed boundary layer, given that the CIMS inlet was located  $\sim 5 \text{ m}$  above the snow surface, which is known to affect gradients of many chemical components, we explore the data using both MISTRA-0D and MISTRA-1D.

A suite of model runs were performed using the MISTRA 0-D model employing different halogen flux parameterisations in an attempt to simulate observations on this day, with all bromine released as a surface flux of Br<sub>2</sub>.

To overcome photolytic destruction of Br<sub>2</sub>, and maintain the observed mixing ratio of  $\sim 5 \text{ pptv}$  around solar noon, would require a Br<sub>2</sub> emission of  $\sim 1 \times 10^{10} \text{ molecules cm}^{-2} \text{ s}^{-1}$  into a well mixed 200 m high boundary layer. This is considerably larger than the release of Br<sub>2</sub> to the atmosphere of  $\sim 6 \times 10^7$  to  $\sim 1.8 \times 10^8 \text{ molecules cm}^{-2} \text{ s}^{-1}$  simulated by Toyota et al. (2011) for the Arctic spring using a 3-D model, and an order of magnitude higher than the  $1 \times 10^9 \text{ molecules cm}^{-2} \text{ s}^{-1}$  used in a 1-D model study of BL halogens in the spring at Halley by Saiz-Lopez et al. (2008). We ran a simulation where this large persistent flux of Br<sub>2</sub> was released over each 24 h period of the model run, in an attempt to explain the daytime Br<sub>2</sub> and BrCl mixing ratio. Although we were able to reproduce the observed daytime mixing ratio of Br<sub>2</sub>, the nighttime values were more than an order of magnitude larger than observed at Halley. The large emission of Br<sub>2</sub> also led to near complete O<sub>3</sub> destruction immediately after the solar zenith angle (SZA) fell below  $88.9^\circ$  (model “sunrise”) on the first day. We then ran the 0-D model with an imposed diurnally varying Br<sub>2</sub> flux, which we coupled to the SZA. Again we were able to reproduce the daytime Br<sub>2</sub> observations (as well as BrCl), but even with no emissions at nighttime Br<sub>2</sub> mixing ratios were more than double the observed value (and BrCl was an order of magnitude larger than observed). Neither of these model simulations was able to reproduce results comparable to both daytime and nighttime Br<sub>2</sub>, BrCl or BrO observations.

In the final 0-D model calculation, we derived the flux of bromine required to achieve the nighttime maximum Br<sub>2</sub> mixing ratio for 6 September 2007 according to the amount of time an air parcel had spent over newly-forming sea ice, which is the expected source region of bromine. This was determined from HYSPLIT back trajectories and sea ice maps (see Fig. 2). Back trajectories run every 2 h for the 24 h period covering 6 September all show a similar path over the newly forming sea-ice in Precious Bay. We assumed a constant emission of Br<sub>2</sub> from the sea-ice zone, and simulated this by release of a steady Br<sub>2</sub> flux over this 24 h period. A flux of  $8 \times 10^7 \text{ molecules cm}^{-2} \text{ s}^{-1}$  was required to reproduce the nighttime halogen measurements at Halley during this event. This flux is in line with that simulated by Toyota et al. (2011), but much smaller than the flux set by Saiz-Lopez et al. (2008).

Figure 3a and b show both the observations of Br<sub>2</sub> and BrCl and their equivalent modelled output from MISTRA-0D for the latter flux experiment described above. It is immediately evident that there are several clear differences between the basic model output and the observations. Firstly, according to the model, daytime mixing ratios of both Br<sub>2</sub> and BrCl should be zero, but the measurements show a clear daytime signal for both Br<sub>2</sub> and BrCl. And secondly, observations of BrCl show a first peak around noon, followed by a second peak around 18:00, while the model only simulates a single peak. In light of the potential HOBr interferent,

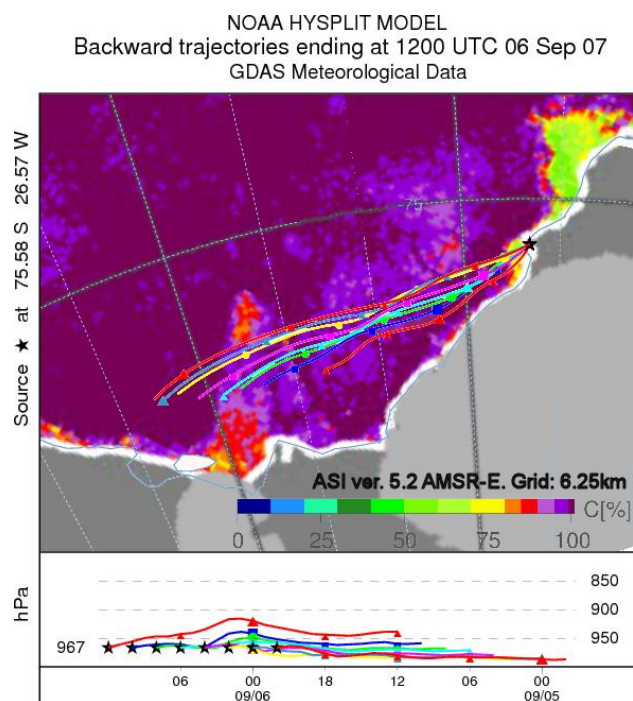


**Fig. 2.** 2-day back trajectories showing air parcel history (location and atmospheric pressure) prior to arrival at Halley on 6 September 2007 overlaid on an AMSR-E image of percentage sea-ice cover. The star marks the position of Halley, and the symbols mark 6-hourly intervals.

model output was re-plotted, incorporating a proportion of modelled HOBr into both modelled Br<sub>2</sub> and modelled BrCl. The results are shown in Fig. 3c and d. Inclusion of this assumed “HOBr interferent” clearly improved agreement between the model and measurements in terms of the daytime mixing ratio amount. Further, for BrCl, inclusion of the artefact yielded a double peak, as observed in the measurements due to the presence of HOBr during the day and possibly early hours of the night.

The initial assumption in the above calculations, regarding the MISTRA 0-D simulations being non height-specific does not take into account vertical gradients such as those introduced by any snowpack emissions. To assess this influence, we used the MISTRA 1-D model to reproduce the BL structure as characterised by the meteorological measurements from Halley. We used the measurements from both the met mast and sodar instrument to initialise the meteorology for these 1-D runs, and initialised the chemistry as for the 0-D simulations. When we used the same Br<sub>2</sub> flux as above, of  $8 \times 10^7$  molecules  $\text{cm}^{-2} \text{s}^{-1}$ , the mixing ratios of Br<sub>2</sub> in the model level corresponding to 4.5–7.5 m above the snow surface were higher than for the 0-D simulations and did not reproduce the measurements. We found that reducing the Br<sub>2</sub> emission slightly to  $6 \times 10^7$  molecules  $\text{cm}^{-2} \text{s}^{-1}$  (the lowest flux derived by Toyota et al., 2011), the model was better

able to reproduce the measured Br<sub>2</sub> for the model level representing 4.5–7.5 m in height (see Fig. 3e and f). This is in line with what we would expect given that in the model Br<sub>2</sub> is emitted from the surface, leading to higher mixing ratios near the surface and dropping off as the distance to the surface increases. While we were not able to reproduce the daytime Br<sub>2</sub> and BrCl measurements in their entirety with the 1-D runs, Fig. 3e and f again show that inclusion of a proportion of modelled HOBr into both Br<sub>2</sub> and BrCl significantly improved agreement with the daytime observations.

Thus the results from both the 0-D and 1-D MISTRA model simulations are consistent with an artefact representing a conversion of HOBr to Br<sub>2</sub> of the order of several tens of percent, with that for HOBr to BrCl being noticeably less but non-negligible. This conclusion is in line with Liao et al. (2012b), who corrected their hourly-averaged diurnal profiles of Br<sub>2</sub> and HOBr observed at Barrow assuming 20 % conversion in the inlet.

During their field observations at Barrow, Liao et al. (2012b) only observed HOBr above detection limits when  $J_{\text{Br}_2} > 0$ . These observations are consistent with theory – no sources of HOBr at night are known for polar regions as all known production pathways require photolytic reactions. Therefore it is reasonable to assume that no HOBr is available for conversion to Br<sub>2</sub> at night. However, as there are no coincident HOBr measurements from Halley, clearly this means that there is still some uncertainty in the influence of HOBr for the Halley case. Nonetheless, for the purposes of this work, and given the evidence for an artefact in CIMS daytime measurements of Br<sub>2</sub> and BrCl caused by conversion of HOBr on the inlet, all Halley plots (Figs. 1, 4, 7, and 9) are colour coded to differentiate between daytime ( $J_{\text{NO}_2} > 0$ ) and nighttime ( $J_{\text{NO}_2} = 0$ ) observations of Br<sub>2</sub> and BrCl, showing all daytime measurements in black.

### 3.2 Br<sub>2</sub>, BrCl and BrO timeseries

Although this was a year round measurement campaign at Halley, the CIMS instrument was only configured for detection of Br<sub>2</sub>, BrCl and BrO for specific periods. Here we focus on a measurement period in austral spring, from 12 August to 18 September 2007, a time which, according to previous work at Halley (Saiz-Lopez et al., 2007), is likely to have active bromine chemistry.

The CIMS technique has been used to detect halogens in several previous polar field campaigns (Foster et al., 2001; Spicer et al., 2002; Neuman et al., 2010; Liao et al., 2011a, b, 2012b). In contrast to issues with Br<sub>2</sub> and BrCl observations discussed in Sect. 3.1, a recent comparison of Arctic ground-based observations of BrO made using both a CIMS and a long-path DOAS showed good agreement when air masses were well mixed (Liao et al., 2011b). We therefore assume that all BrO observations made at Halley are interferent-free.

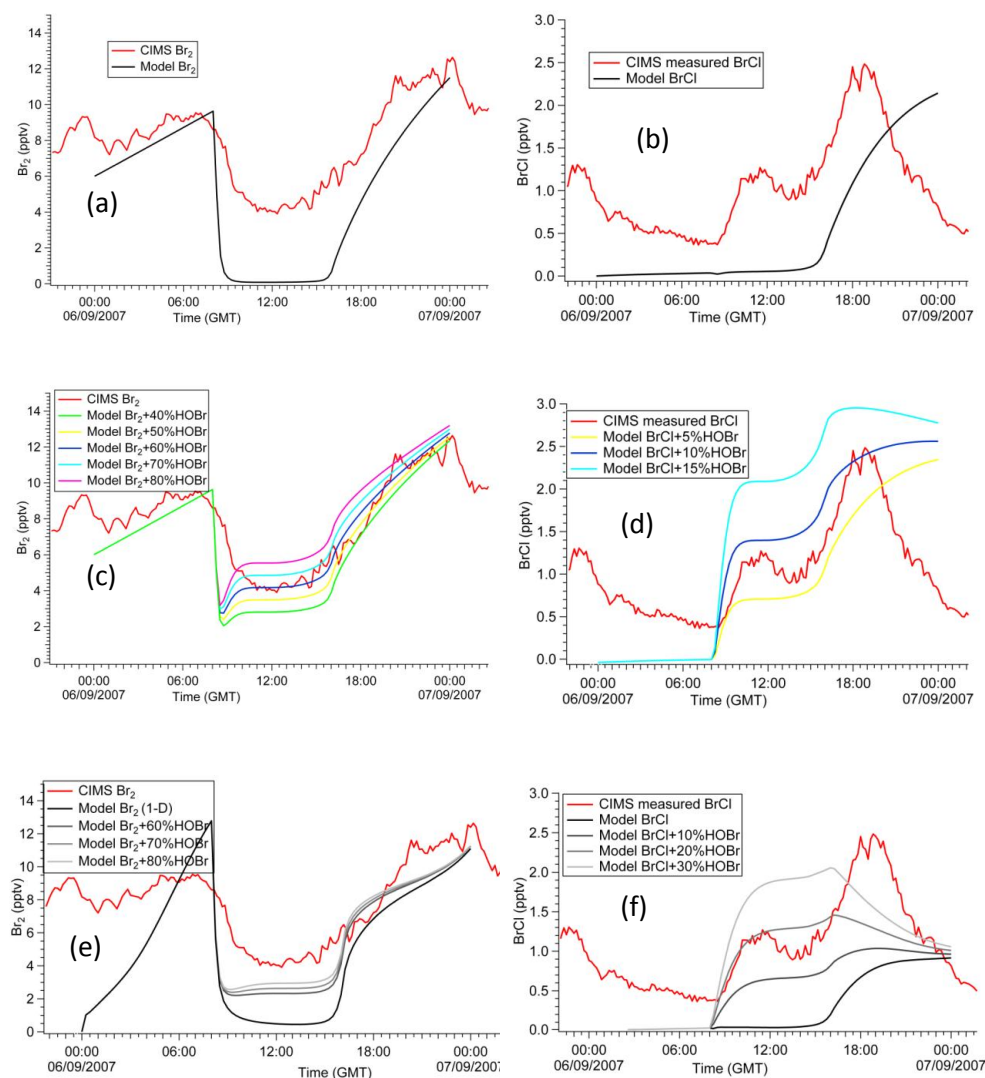


**Fig. 3.** (a) comparison between Br<sub>2</sub> measured with CIMS and that modelled with MISTRA-0D for 6 and 7 September 2007; (b) as for (a) but this time showing BrCl; (c) comparison between Br<sub>2</sub> measured with CIMS, and that modelled with MISTRA-0D, but now with 40 %, 50 %, 60 %, 70 %, and 80 % of model HOBr added to model Br<sub>2</sub>; (d) as for (c) but with 5 %, 10 % and 15 % of model HOBr added to model BrCl; (e) comparison between Br<sub>2</sub> measured with CIMS and that modelled with MISTRA-1D, with 60 %, 70 % and 80 % of model HOBr added to model Br<sub>2</sub>; (f) as for (e) but with 10 %, 20 % and 30 % of model HOBr added to model BrCl. Both 1-D model outputs (e) and (f) correspond to a height of 4.5–7.5 m above the snowpack.

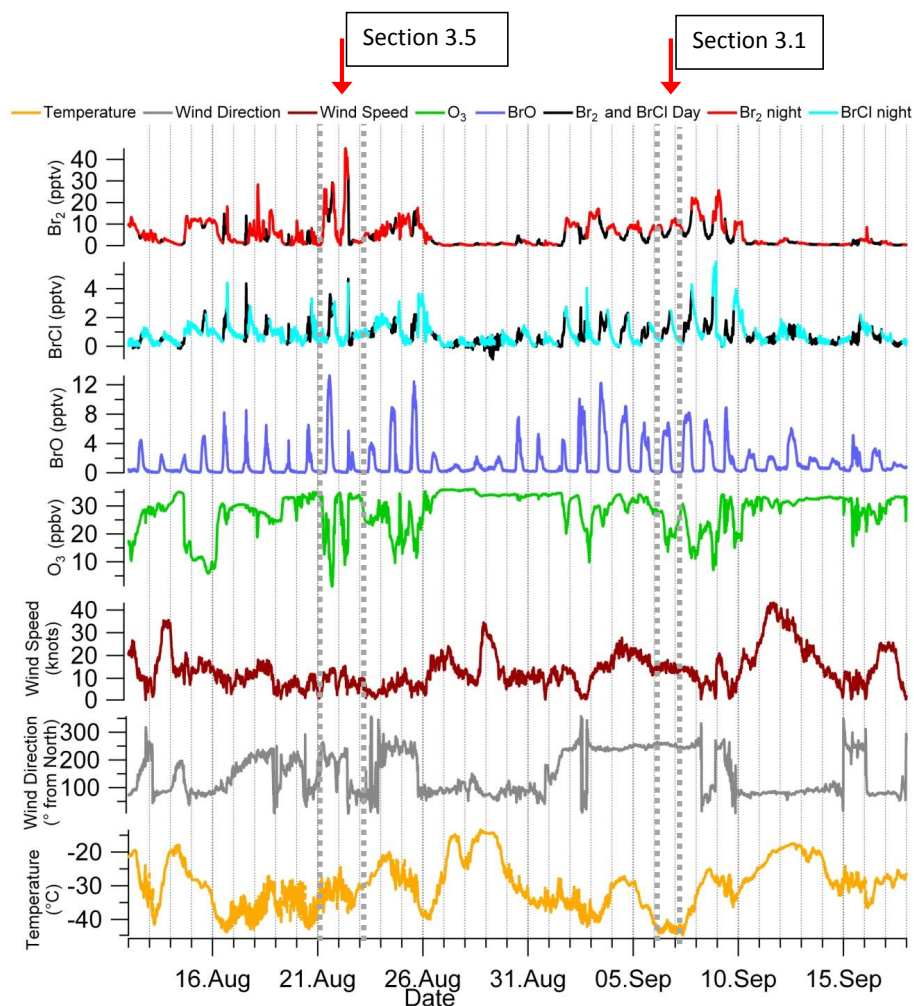
### 3.2.1 Overview of the data

Figure 4 presents the time series of Br<sub>2</sub>, BrCl, BrO and surface O<sub>3</sub> together with concurrent meteorological observations of local wind speed/direction and local temperature for the entire measurement period.

Br<sub>2</sub> mixing ratios vary from below instrument detection limits (refer to Table 1) to a maximum of 45 pptv (observed at night) and BrCl from below detection limits to ~ 6 pptv (at night). As shown in Fig. 4, there is considerable variability in the Br<sub>2</sub> and BrCl observations over the measurement period which is strongly linked to the prevailing meteorology and thus air mass origin. Relatively low and invariant

Br<sub>2</sub> and BrCl is generally associated with easterly winds of continental origin with higher mixing ratios in air masses that have passed over sea ice to the west/south west. Surprisingly, the highest measured mixing ratio of Br<sub>2</sub> and the lowest measured surface ozone, appear to be associated with a long-range transport event where air is arriving at Halley from across the continent via the South Pole, with its last sea ice contact somewhere to the west of the Antarctic Peninsula (discussed in Sect. 3.5)

The range of BrO mixing ratios during the measurement period, from instrumental detection limits to ~ 13 pptv, are in line with previous observations at Halley (Saiz-Lopez et



**Fig. 4.** Overview of measurements at Halley from 12 August to 18 September 2007. Br<sub>2</sub>, BrCl and BrO are shown as 10 min averages; for Br<sub>2</sub> and BrCl, daytime observations are coloured black. Also shown are surface O<sub>3</sub> (10 min averages), local wind speed and direction, and local temperature.

al., 2007) made using a long-path DOAS. The BrO maxima at Halley are less obviously correlated with local wind direction than are Br<sub>2</sub> and BrCl. For example, from 27 August until 1 September, while the prevailing wind direction is easterly (implying continental air), Br<sub>2</sub> and BrCl show little variability, and there is no ODE, BrO maintains a diurnal structure with daily maxima ranging from  $\sim 2$  pptv to  $\sim 7$  pptv. These values are in line with daytime BrO measured previously at Halley in air of continental origin (Saiz-Lopez et al., 2007). The presence of a diurnal variability in BrO throughout the measurement period suggests that some persistent background bromine/ozone chemistry is active during the day, even when air is not approaching from directly across the sea ice zone.

A clear example of such background chemistry occurs on 30 August when  $\sim 7$  pptv of BrO was measured in air arriving at Halley, the highest BrO mixing ratios measured dur-

ing a period of sustained continental origin (Fig. 4). There is little O<sub>3</sub> depletion on this day, but the  $\sim 3$ – $4$  pptv of “Br<sub>2</sub>” measured during daylight is indicative of active bromine chemistry (possibly as HOBr) (see Sect. 3.1). Wind speeds were low ( $\sim 5$  m s<sup>-1</sup>) and local ambient temperature was around  $-30$  °C. The importance of halogen recycling in/on the snowpack is discussed in a model study by Piot and von Glasow (2008), where they varied the percentage re-emission of Br<sub>2</sub>/BrCl in their runs from 0–100%. They found that major ODEs could only be reproduced in their model simulations when the recycling of bromine deposited on snow into gas phase bromine was included. If we therefore assume that recycling of bromine deposited on (or present in) snow is generally occurring at all times in coastal polar regions, the measurements discussed here (30 August 2007) suggest that a cold, stable/stratified BL has led to this build up of several pptv of BrO. Under the same meteorological conditions

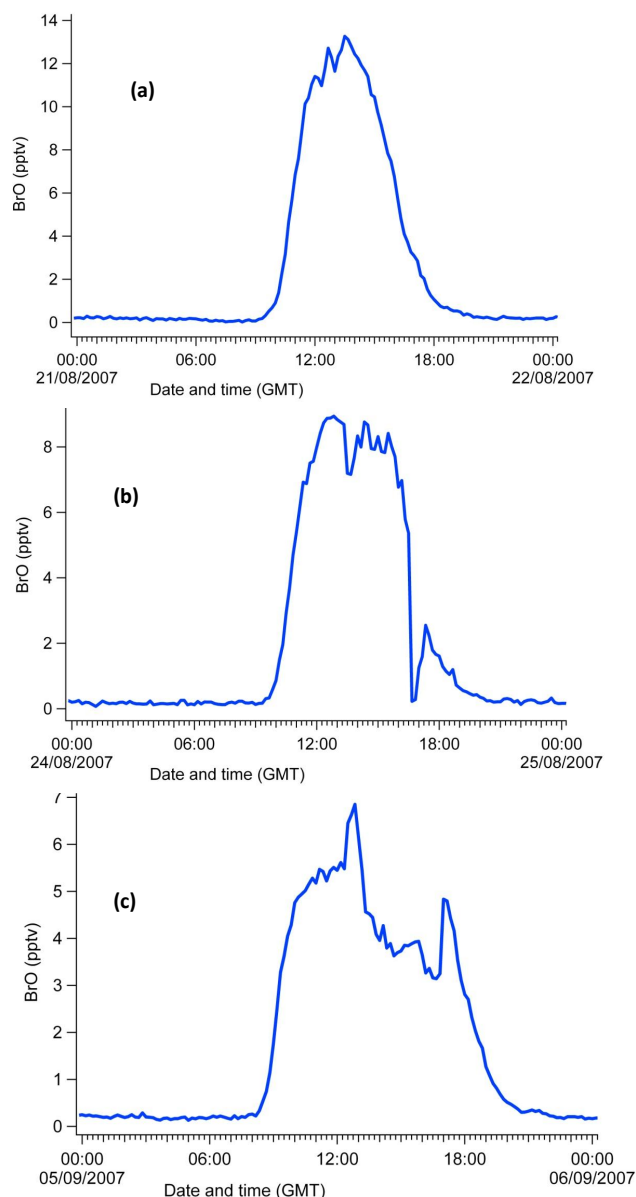


**Fig. 5.** Plots showing diurnal shape of BrO in pptv with time and date on the x-axis. (a) a single peak around noon; (b) a broad flat-topped maximum also around noon; and (c) double peak with maxima shortly after sunrise and shortly before sunset.

on the following day (31 August 2007), we measure up to 5 pptv of BrO. These enhanced BrO mixing ratios measured in air of sustained continental origin suggest release of halogens directly from the snowpack, and their detection at the several pptv level may be dependent on these very specific meteorological conditions.

### 3.2.2 Diurnal variability in BrO, Br<sub>2</sub> and BrCl

BrO exhibits a clear diurnal cycle throughout the period of CIMS observations, with nighttime minima around instru-

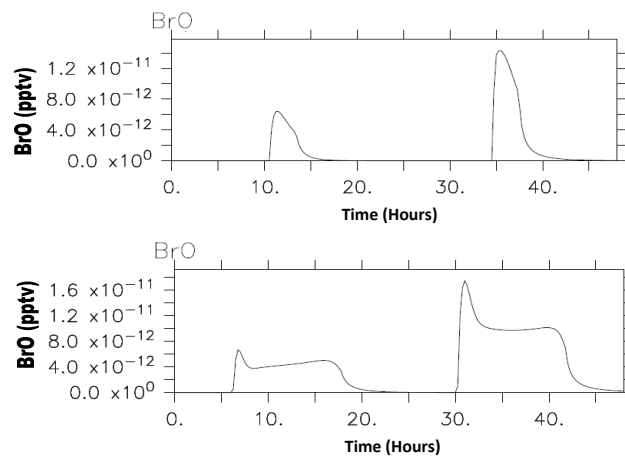


**Fig. 6.** BrO model output from MISTRA 0-D showing (a) a single BrO peak around noon when solar declination is set to represent early spring at Halley; and (b) a double BrO peak with a maximum in the morning and evening, with a noon time minimum when solar declination is set to represent late spring at Halley.

mental detection limits (Fig. 4). The characteristic of the daytime maxima vary from day to day, being either (i) a single peak around noon (Fig. 5a), (ii) a broad flat-topped maximum also around noon (Fig. 5b), or (iii) double peaks with maxima shortly after sunrise and shortly before sunset (Fig. 5c). Such double-peaks were also observed by Pöhler et al. (2010) during springtime measurements in the Amundsen Gulf, and in springtime observations at Barrow, Alaska (Liao et al., 2012b). A model study by von Glasow et al. (2002) also showed this distinct diurnal structure of a BrO minimum around noon, and maxima in the morning and evening. In their model calculations this was caused by differences in the photolysis spectra of O<sub>3</sub> and Br<sub>2</sub>, where Br<sub>2</sub> is more rapidly photolysed in twilight than O<sub>3</sub> due to absorption at longer wavelengths. BrO concentrations are a balance of sources and sinks. The main source of BrO is photolysis of Br<sub>2</sub> followed by reaction of the Br atoms with ozone. The main sink of BrO under polar conditions is reaction with HO<sub>2</sub>. HO<sub>2</sub> itself is photolytically produced by way of O<sub>3</sub> photolysis. At high solar zenith angles (such as morning and evening) BrO is already produced efficiently but the HO<sub>2</sub> only at lower SZAs. Hence the efficiency of the HO<sub>2</sub> sink is highest during the hours around noon causing the dip in BrO mixing ratios around noon in double-peaked profiles or the reduced noon maximum in the flat profiles.

The occurrence of flat-topped maxima and double peak BrO increases at Halley as the spring season progresses away from polar night. To explore this changing BrO diurnal shape as the measurement period progressed, two model simulations were run using MISTRA 0-D (Fig. 6). Figure 6a is a model simulation set with a solar declination angle,  $\varphi$ , representative of the beginning of the measurement period (13 August,  $\varphi = 14.5^\circ$ ) and Fig. 6b with a solar declination

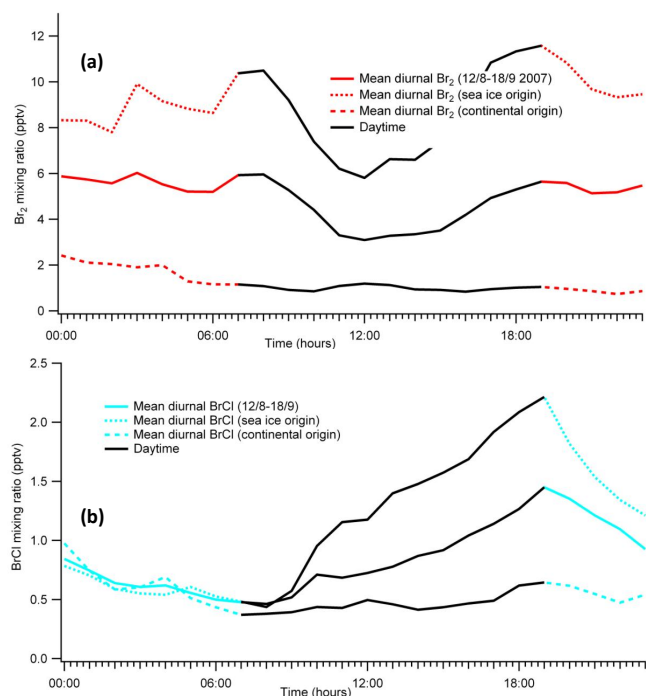


**Fig. 7.** Hourly mean diurnal plots of (a) Br<sub>2</sub>, and (b) BrCl for all the data, and for different source regions (sea-ice zone; continental).

representative of the end of the measurement period (18 September,  $\varphi = 1.9^\circ$ ). Figure 6a clearly shows a single BrO peak around noon. At this time of year days are very short, the SZA is very high and O<sub>3</sub> UV photolysis is low, and insufficient HO<sub>2</sub> is produced to reduce BrO mixing ratios significantly to give a noon minimum. The BrO mixing ratios in Fig. 6b, however, show a clear morning peak followed by a minimum around noon and rising again to a second less-well-defined maximum just prior to sunset. Here days are long enough to allow sufficiently low noon-time SZAs, implying that sufficient HO<sub>2</sub> is produced to reduce BrO mixing ratios leading to a minimum around noon.

Figure 7 shows the hourly mean diurnal variability for the entire measurement period for Br<sub>2</sub> (Fig. 7a) and BrCl (Fig. 7b), the three lines on each plot representing (i) all data, (ii) air with a sea ice zone origin, and (iii) air with a continental origin (as determined from local wind direction). Daytime components of Br<sub>2</sub> and BrCl are indicated by black lines. The data immediately demonstrate the importance of filtering according to air mass origin when calculating averaged diurnal cycles for these halogen species from coastal observations.

Focussing on the hours from midnight to dawn, we note (Fig. 7a) that the hourly-averaged Br<sub>2</sub> mixing ratios increase over this time period in air with a sea ice zone origin. The potential for outgassing of Br<sub>2</sub> from sea salt aerosol at night has been demonstrated in modelling calculations by von Glasow et al. (2002), driven by gas-aqueous partitioning from gas-phase BrCl. Such increases in Br<sub>2</sub> are not evident in air with

a continental origin (Fig. 7a), where the Br<sub>2</sub> mixing ratios decrease between midnight and dawn.

The reduction in hourly-averaged BrCl between midnight and dawn in sea ice zone air (Fig. 7b) is consistent with uptake and re-partitioning to Br<sub>2</sub> (although not sufficient to account for all the observed Br<sub>2</sub> increase). It is somewhat surprising, however, that BrCl mixing ratios decrease also in air with a continental origin, particularly given that Br<sub>2</sub> mixing ratios in the same air masses also decrease. The observations suggest uptake of both Br<sub>2</sub> and BrCl onto surfaces at night.

### 3.2.3 Period of sustained surface O<sub>3</sub> depletion

From 14 to 16 August the most sustained (> 24 h) ODE of the whole measurement period was observed. O<sub>3</sub> mixing ratios dropped from a background of 33 ppbv to 18 ppbv (a change in 15 ppbv) over a 20 min period (15:20–15:40) on 14 August and continued to fall to a minimum of 6 ppbv. This rapid change in [O<sub>3</sub>] suggests transport of an ozone depleted air mass to Halley. ECMWF ERA Interim re-analysis plots of mean surface pressure and 10 m wind speed vectors indicate that a low pressure system was present over the Weddell Sea sea ice for several days before coming into contact with Halley (not shown). At noon on 13 August, 10 m wind speeds were > 12 m s<sup>-1</sup> over the central Weddell Sea and > 16 m s<sup>-1</sup> at the northern Weddell Sea near the sea ice edge. Wind speeds > 12 m s<sup>-1</sup> can create “blowing snow” conditions (Jones et al., 2009), and Yang et al. (2008) suggest lofted snow on sea ice can give rise to enhanced tropospheric bromine which can then react to destroy ozone. As the low pressure system moved over Halley wind speeds dropped to < 4 m s<sup>-1</sup>. This suggests that the high wind speeds (> 16 m s<sup>-1</sup>) observed at the northern Weddell Sea sea ice zone on 13 August could be the driver of the ODE measured at Halley on 14–16 August. The air mass is first depleted in ozone, then transported to Halley where the wind speeds drop and the ozone depleted air mass resides over Halley for > 24 h. There is then a rise in O<sub>3</sub> from 10–25 ppbv from 04:00–06:00 on 16 August, signalling the end of the ODE. This replenishment of O<sub>3</sub> may be caused by a shift in the balance of air flow from sea ice zone (low pressure system) and from the continent (orographic flow).

### 3.3 Br<sub>2</sub> : BrCl ratios

As discussed in Sect. 1, air masses arriving at Halley during spring generally have either a continental or a sea ice zone influence. We have discussed the potential importance of the sea ice zone for halogen release and ozone depletion, but here we will look at a more detailed picture of the influence these different source regions have on Br<sub>2</sub> : BrCl ratios.

Figure 8 shows the ratio of Br<sub>2</sub> : BrCl derived from the Halley nighttime observations, and colour coded for local wind direction. There is considerable variability in the ratio much of which is clearly associated with wind direction

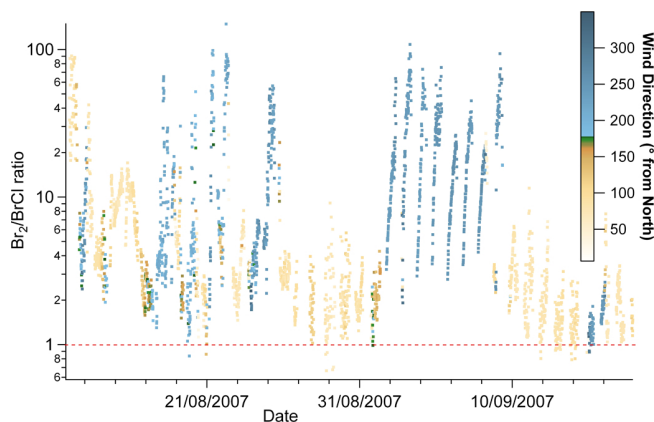


**Fig. 8.** Nighttime ratio of Br<sub>2</sub> : BrCl throughout the measurement period on a log scale. The colour coding indicates local wind direction (blues indicate sea ice zone origin; oranges indicate continental origin), emphasising the influence of air mass origin on the calculated ratio. A red dashed line is drawn at a ratio of one to highlight the small number of values found below it.

and thereby halogen source region. For example, from 10 September onwards, the ratio is very low, as are the mixing ratios of both Br<sub>2</sub> and BrCl (see Fig. 4), resulting from air masses with little/no sea ice contact. These air masses have little/no ozone depletion. In contrast, air masses with an origin from the sea ice zone (e.g. 3 to 8 September) which are depleted in ozone and enhanced in halogens, have a Br<sub>2</sub> : BrCl ratio clearly in favour of Br<sub>2</sub> (~2–100). On a very few occasions the Br<sub>2</sub> : BrCl ratio drops below 1 (red dashed line in Fig. 8). Such low ratios can be attributed to the very low (near detection limit) mixing ratios of both Br<sub>2</sub> and BrCl; use of a 3 $\sigma$  LOD filter rather than a 2 $\sigma$  filter (Table 1) would remove these points.

From 10 to 14 September, our data show a decrease in the Br<sub>2</sub> : BrCl ratio with time since the last exposure to sea ice (Fig. 8). As discussed in Sect. 3.2.1, recycling of bromine deposited on the snowpack can be a source of gas phase bromine. One explanation for this decrease in the Br<sub>2</sub> : BrCl ratio could be that the availability of bromine previously deposited to the snowpack reduces over time, leading to less recycling into gas phase bromine.

### 3.4 Comparison with Arctic Br<sub>2</sub>, BrCl and BrO observations

High resolution ground-based measurements of Br<sub>2</sub> and BrCl were previously made in the Arctic as part of the Alert Polar Sunrise Experiment (PSE) (Foster et al., 2001; Spicer et al., 2002). These measurements were conducted prior to first direct sunlight, and continued for a further two weeks after polar sunrise. In the period following first direct sunlight, Spicer et al. (2002) reported Br<sub>2</sub> mixing ratios at Alert that ranged from instrumental detection limits to 27 pptv (which we note was measured when solar irradiance was 0 W m<sup>-2</sup>, i.e. night-

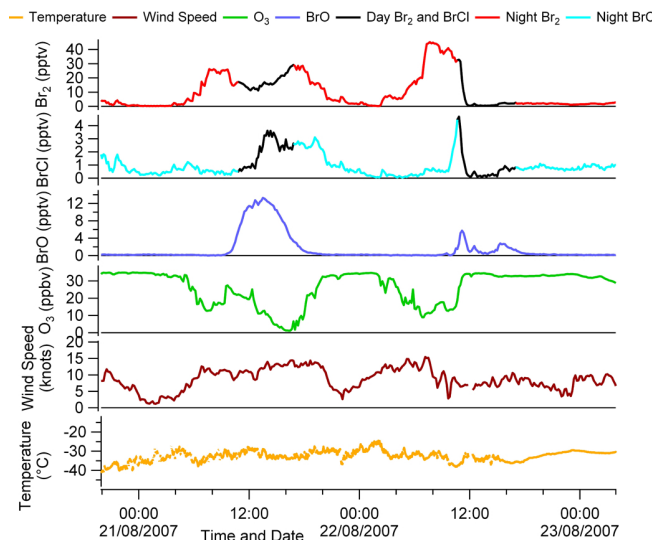


**Fig. 9.** Wind speed, temperature, surface O<sub>3</sub> and CIMS Br<sub>2</sub>, BrCl and BrO measurements from Halley on 21 and 22 August 2007.

time observations). For the same period at Alert, Foster et al. (2001) reported BrCl mixing ratios ranging from detection limits to ~35 pptv, although without showing whether this was daytime or nighttime data. However, Spicer et al. (2002) measured daytime (i.e. solar irradiance > 0 W m<sup>-2</sup>) BrCl up to ~25 pptv, and nighttime (i.e. solar irradiance = 0 W m<sup>-2</sup>) BrCl up to ~18 pptv. Their nighttime BrCl is considerably larger than was observed at Halley, where nighttime BrCl mixing ratios were never greater than 6 pptv. The data from Spicer et al. (2002) therefore suggest that BrCl in the Arctic can reach considerably greater mixing ratios than were measured at Halley. Furthermore, when 18 pptv of BrCl were measured at Alert, the coincident Br<sub>2</sub> measured was only ~4 pptv, i.e. a Br<sub>2</sub> : BrCl ratio of ~0.2 – considerably less than observed at Halley. In general Foster et al. (2001) describe the measured ratio of Br<sub>2</sub> to BrCl in the air to be ~1, whereas at Halley, the ratio was almost always significantly greater than 1 (see Sect. 3.3). The measurements at Alert were made using a similar CIMS technique to that at Halley, but with a ~9 m long teflon inlet (J. Bottenheim, personal communication, 2012), which raises the question of whether they were also subject to an inlet artefact in daytime Br<sub>2</sub> and BrCl observations discussed in Sect. 3.1. If so, this would likely affect both the recorded mixing ratios and ratios.

A more recent study by Liao et al. (2012b), reports measurements of BrO, Br<sub>2</sub> and HOBr made using a modified CIMS technique at Barrow, Alaska, in spring 2009. Their observations show a BrO maximum of > 30 pptv, more than double the observed maximum at Halley of 13 pptv. Maxima in Br<sub>2</sub> at the two stations are very similar, with 46 pptv at Barrow and 45 pptv observed at Halley.

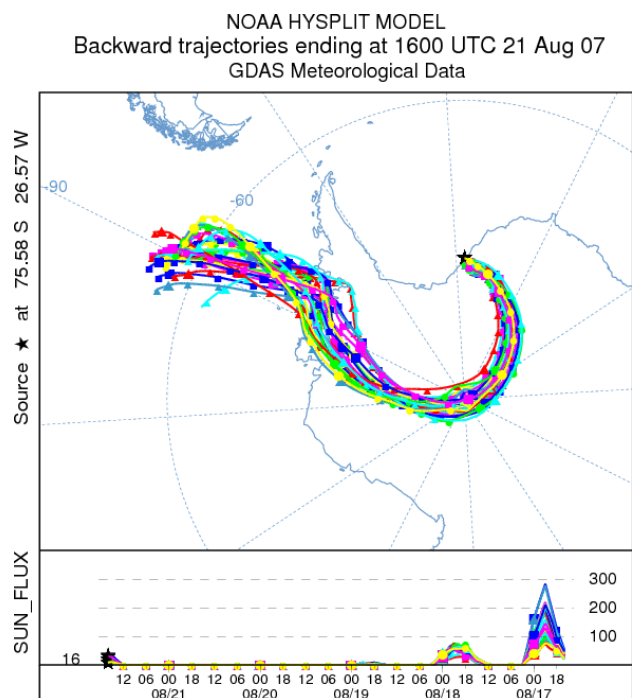


**Fig. 10.** 5-day HYSPLIT Ensemble back trajectory from Halley. Included is a measure of “Downward Solar Radiation Flux ( $\text{W m}^{-2}$ )” to indicate when the air parcel last experienced light.

### 3.5 Long range transport (in darkness) of a halogen enriched, ozone-depleted, air mass

Over a two day period from 21–22 August an intriguing event was observed at Halley, with the lowest measured [ $\text{O}_3$ ] throughout the entire period of observations and the highest mixing ratios of [ $\text{Br}_2$ ] and [ $\text{BrO}$ ] (Fig. 9). The highest measured [ $\text{Br}_2$ ] of the whole spring period occurred after midnight on 22 August, so is not likely to be influenced by the HOBr interferent (discussed in Sect. 3.1). HYSPLIT back trajectories suggest that this ozone depleted air mass had arrived at Halley having travelled across the continent of Antarctica from the Bellingshausen Sea, to the west of the Antarctic Peninsula (Fig. 10). As shown by the lower panel of Fig. 10, the air mass had travelled in darkness for the previous 3 1/2 days with no possibility of photochemical reactions taking place. AMSR-E maps (not shown) show open water leads, with associated sea-ice formation processes, at the coastal edge of the Bellingshausen in the region of the air mass trajectories. This area could be seen as the main source of halogen for the air mass, but it could also be argued that the furthest edge of the sea is the greatest halogen source. A third possibility is that these source regions may have some influence, but what we see is also the result of chemistry in the near-coastal environment at Halley.

Figure 11 shows surface ozone measurements from South Pole from 1–31 August 2007. The outstanding feature is the

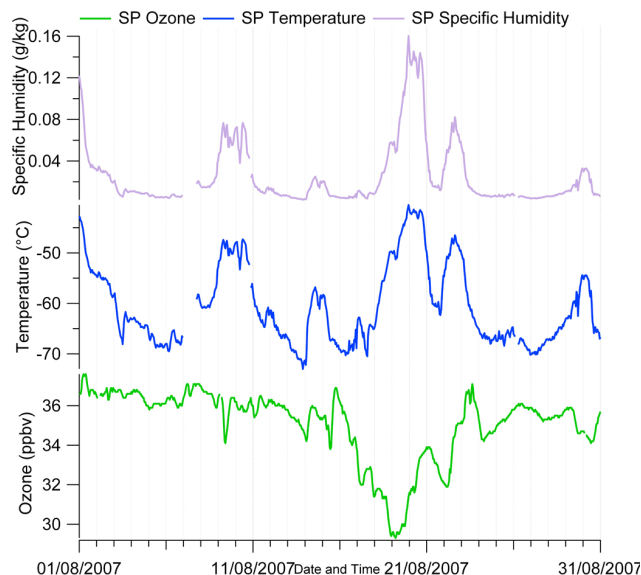


**Fig. 11.** South Pole surface ozone, temperature and specific humidity, from 1–31 August 2007.

drop in ozone that occurs on 19–20 August. The back trajectories shown on Fig. 10 indicate that the low-ozone air arriving at Halley on 21 August had passed over South Pole on 19–20 August. While the drop in ozone at South Pole is modest compared with the Halley observations, the HYSPLIT trajectories suggest that the Halley air mass did not skirt the surface, but travelled at some height ( $> 1000$  m) over South Pole. The drop in surface ozone of 7–8 ppb on 19 August is consistent with an ozone depleted air mass following this trajectory over South Pole with only a small influence being evident at the surface. Unfortunately no ozone sonde was launched from South Pole on this day, from which the profile of ozone could be seen. However, data from South Pole of temperature and specific humidity both show significant increases, consistent with passage of marine air. Further, Bromwich et al. (1996) suggest that passage of air across the continent along this route is not uncommon.

In an attempt to understand the halogen chemistry occurring during this period of darkness as the air mass traversed the continent, a run in MISTRA-0D was set up to recreate the conditions the air mass would see (Fig. 12). An initial mixing ratio for  $\text{Br}_2$  was set at 40 pptv, with the majority of the remaining parameters set for a typical Halley model run. HYSPLIT trajectories were used to determine the length of run required, and the influence of light on the air mass. The result is shown in Fig. 12. It is clear that the initial influence of sunlight is of vital importance in the partitioning of halogen species between  $\text{Br}_2$  and  $\text{BrCl}$ , but it appears that the lack of photolysis thereafter effectively “stalls” the ozone depleting reactions. This implies that the majority of ozone depletion would have to occur prior to the period of darkness, although there is some photolytic influence near the end

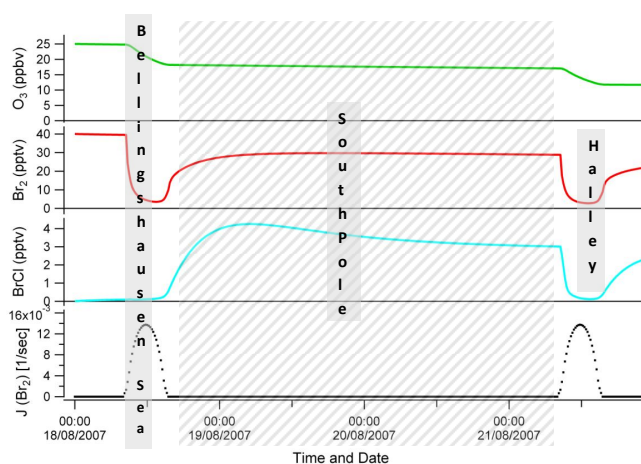


**Fig. 12.** MISTRA 0-D run 4 days in length showing [Br<sub>2</sub>], [BrCl], [O<sub>3</sub>] and  $J(\text{Br}_2)$  model output. Only the first and last of those days under the influence of sunlight (darkness is highlighted with the hashed grey box). Mixing ratio on the left axis, and time in hours since the start of the run along the bottom. The location of the air mass is highlighted at key stages of its transcontinental path.

of the run. Although the model run does not show complete ozone depletion as observed at Halley, the run does highlight the transport of the depleted air mass in the dark. We also note that the final [Br<sub>2</sub>] and [BrCl] output from the model run is comparable to the halogen observations from Halley on 21 August 2007 (see Fig. 9).

#### 4 Conclusions

We report the first high temporal resolution measurements of BrO, Br<sub>2</sub> and BrCl in coastal Antarctica, made during spring 2007 using a CIMS instrument. The previously-reported artefact, arising from an inlet conversion of HOBr and affecting Br<sub>2</sub> observations, may also be apparent in our data; we also suggest there may be a minor artefact on BrCl. This is not, however, a fundamental instrument restriction and refers more to our specific sampling methodology. Results from the MISTRA 0-D and 1-D model runs indicate that the artefact represents a conversion of HOBr to Br<sub>2</sub> of the order of several tens of percent, while that for HOBr to BrCl is less but non-negligible. Conclusions can be drawn about the Br<sub>2</sub> and BrCl observations by restricting focus to their nighttime results only. Mixing ratios of BrO, Br<sub>2</sub> and BrCl ranged from instrumental detection limits to 13 pptv (daytime), 45 pptv (nighttime), and 6 pptv (nighttime), respectively. It is interesting to note that as the spring season progressed, the diurnal shape of BrO changed from a sharp single peak, to a broad/flat-topped peak and finally to a double peak with BrO maxima in the morning and evening along with noon time minima. This suite of Antarctic data provides the first analogue to similar measurements made in the Arc-

tic. Previously-reported nighttime maxima for Br<sub>2</sub> (46 pptv at Barrow, Liao et al., 2012b and 27 pptv at Alert, Spicer et al., 2002) are in line with the Halley observations. Arctic nighttime BrCl mixing ratios up to 18 pptv (Spicer et al., 2002), however, are considerably larger than observed at Halley. Further, ratios of Br<sub>2</sub>:BrCl at Alert appear to be lower than measured at Halley, where air masses with an origin from the sea ice zone have a ratio in favour of Br<sub>2</sub> and are never less than 1 if filtered using a 3 $\sigma$  LOD. An unusual event of trans-continental air mass transport in darkness was associated with severe surface ozone depletion observed at Halley. Model calculations were consistent with the halogen source region being to the west of the Antarctic Peninsula, with the air mass having spent 3 1/2 days in complete darkness crossing the continent prior to arrival at Halley. Not only was this air mass strongly depleted in O<sub>3</sub>, it was also the source of both the highest measured [Br<sub>2</sub>] and [BrO] for the whole measurement period. Although there are several possible explanations for these measurements (discussed in Sect. 3.5), the evidence suggests that this ozone depleted, halogen-enriched air mass was transported over thousands of kilometres in complete darkness with its halogen source being the sea ice zone on the West side of the Antarctic Peninsula.

*Acknowledgements.* The authors gratefully acknowledge the NOAA Air Resources Laboratory (ARL) for the provision of the HYSPLIT transport and dispersion model and/or READY website (<http://www.arl.noaa.gov/ready.php>) used in this publication.

Surface ozone and meteorological data was provided by NOAA's Climate Monitoring and Diagnostics Laboratory (CMDL) via their data archive <http://www.cmdl.noaa.gov/info/ftpdata.html>.

We thank Tony Phillips of the British Antarctic Survey for giving us access to an experimental service providing web access to IDL-based PP plotting routines of ECMWF operational analysis data.

This study is part of the British Antarctic Survey Polar Science for Planet Earth programme. Zak Buys' studentship was funded by the Natural Environment Research Council through a BAS Algorithm grant.

Edited by: J. W. Bottenheim

#### References

- Abbatt, J. P. D.: Heterogeneous reaction of HOBr with HBr and HCl on ice surfaces at 228 K, *Geophys. Res. Lett.*, 21, 665–668, doi:10.1029/94GL00775, 1994.
- Abbatt, J. P. D., Thomas, J. L., Abrahamsson, K., Boxe, C., Granfors, A., Jones, A. E., King, M. D., Saiz-Lopez, A., Shepson, P. B., Sodeau, J., Toohey, D. W., Toubin, C., von Glasow, R., Wren, S. N., and Yang, X.: Halogen activation via interactions with environmental ice and snow in the polar lower troposphere and other regions, *Atmos. Chem. Phys.*, 12, 6237–6271, doi:10.5194/acp-12-6237-2012, 2012.

- Adams, J. W., Holmes, N. S., and Crowley, J. N.: Uptake and reaction of HOBr on frozen and dry NaCl/NaBr surfaces between 253 and 233 K, *Atmos. Chem. Phys.*, 2, 79–91, doi:10.5194/acp-2-79-2002, 2002.
- Anderson, P. S. and Neff, W. D.: Boundary layer physics over snow and ice, *Atmos. Chem. Phys.*, 8, 3563–3582, doi:10.5194/acp-8-3563-2008, 2008.
- Arnold, S. T. and Viggiano, A. A.: Turbulent ion flow tube study of the cluster-mediated reactions of SF<sub>6</sub><sup>-</sup> with H<sub>2</sub>O, CH<sub>3</sub>OH, and C<sub>2</sub>H<sub>5</sub>OH from 50 to 500 torr, *J. Phys. Chem. A*, 105, 3527–3531, 2001.
- Barrie, L. A., Bottenheim, J. W., Schnell, R. C., Crutzen, P. J., and Rasmussen, R. A.: Ozone Destruction and Photochemical-Reactions at Polar Sunrise in the Lower Arctic Atmosphere, *Nature*, 334, 138–141, 1988.
- Berresheim, H., Elste, T., Plass-Dulmer, C., Eisele, F. L., and Tanner, D. J.: Chemical ionization mass spectrometer for long-term measurements of atmospheric OH and H<sub>2</sub>SO<sub>4</sub>, *Int. J. Mass Spectrom.*, 202, 91–109, 2000.
- Bottenheim, J. W., Gallant, A. G., and Brice, K. A.: Measurements of NO<sub>y</sub> Species and O<sub>3</sub> at 82° N Latitude, *Geophys. Res. Lett.*, 13, 113–116, 1986.
- Bromwich, D. H., Carrasco J. F., and Turner J.: A Downward Developing Mesoscale Cyclone Over the Ross Ice Shelf During Winter, *Global Atmos. Ocean Syst.*, 4, 125–147, 1996.
- Damian, V., Sandu, A., Damien, M., Potra, F., and Carmichael, G. R.: The kinetic preprocessor kpp – a software environment for solving chemical kinetics, *Comp. Chem. Eng.*, 26, 1567–1579, 2002.
- Draxler, R. R. and Rolph, G. D.: HYSPLIT (HYbrid Single-Particle Lagrangian Integrated Trajectory) Model access via NOAA ARL READY Website (<http://ready.arl.noaa.gov/HYSPLIT.php>), NOAA Air Resources Laboratory, Silver Spring, MD, 2012.
- Fickert, S., Adams, J. W., and Crowley, J. N.: Activation of Br<sub>2</sub> and BrCl via uptake of HOBr onto aqueous salt solutions, *J. Geophys. Res.*, 104, 23719–23727, doi:10.1029/1999JD900359, 1999.
- Foster, K. L., Plastring, R. A., Bottenheim, J. W., Shepson, P. B., Finlayson-Pitts, B. J., and Spicer, C. W.: The role of Br<sub>2</sub> and BrCl in surface ozone destruction at polar sunrise, *Science*, 291, 471–474, 2001.
- Gilman, J. B., Burkhart, J. F., Lerner, B. M., Williams, E. J., Kuster, W. C., Goldan, P. D., Murphy, P. C., Warneke, C., Fowler, C., Montzka, S. A., Miller, B. R., Miller, L., Oltmans, S. J., Ryerson, T. B., Cooper, O. R., Stohl, A., and de Gouw, J. A.: Ozone variability and halogen oxidation within the Arctic and sub-Arctic springtime boundary layer, *Atmos. Chem. Phys.*, 10, 10223–10236, doi:10.5194/acp-10-10223-2010, 2010.
- Huey, L. G., Hanson, D. R., and Howard, C. J.: Reactions of SF<sub>6</sub><sup>-</sup> and I<sup>-</sup> with Atmospheric Trace Gases, *J. Phys. Chem.*, 99, 5001–5008, doi:10.1021/j100014a021, 1995.
- Huey, L. G., Dunlea, E. J., Lovejoy, E. R., Hanson, D. R., Norton, R. B., Fehsenfeld, F. C., and Howard, C. J.: Fast time response measurements of HNO<sub>3</sub> in air with a chemical ionization mass spectrometer, *J. Geophys. Res.-Atmos.*, 103, 3355–3360, 1998.
- Huey, L. G., Tanner, D. J., Slusher, D. L., Dibb, J. E., Arimoto, R., Chen, G., Davis, D., Buhr, M. P., Nowak, J. B., Mauldin, R. L., Eisele, F. L., and Kosciuch, E.: CIMS measurements of HNO<sub>3</sub> and SO<sub>2</sub> at the South Pole during ISCAT 2000, *Atmos. Environ.*, 38, 5411–5421, doi:10.1016/j.atmosenv.2004.04.037, 2004.
- Jacobi, H.-W., Morin, S., and Bottenheim, J. W.: Observation of widespread depletion of ozone in the springtime boundary layer of the central Arctic linked to mesoscale synoptic conditions, *J. Geophys. Res.*, 115, D17302, doi:10.1029/2010JD013940, 2010.
- Jones, A. E., Anderson, P. S., Wolff, E. W., Turner, J., Rankin, A. M., and Colwell, S. R.: A role for newly forming sea ice in springtime polar tropospheric ozone loss? Observational evidence from Halley station, Antarctica, *J. Geophys. Res.*, 111, D08306, doi:10.1029/2005JD006566, 2006.
- Jones, A. E., Wolff, E. W., Salmon, R. A., Bauguitte, S. J.-B., Roscoe, H. K., Anderson, P. S., Ames, D., Clemmitshaw, K. C., Fleming, Z. L., Bloss, W. J., Heard, D. E., Lee, J. D., Read, K. A., Hamer, P., Shallcross, D. E., Jackson, A. V., Walker, S. L., Lewis, A. C., Mills, G. P., Plane, J. M. C., Saiz-Lopez, A., Sturges, W. T., and Worton, D. R.: Chemistry of the Antarctic Boundary Layer and the Interface with Snow: an overview of the CHABLIS campaign, *Atmos. Chem. Phys.*, 8, 3789–3803, doi:10.5194/acp-8-3789-2008, 2008.
- Jones, A. E., Anderson, P. S., Begoin, M., Brough, N., Hutterli, M. A., Marshall, G. J., Richter, A., Roscoe, H. K., and Wolff, E. W.: BrO, blizzards, and drivers of polar tropospheric ozone depletion events, *Atmos. Chem. Phys.*, 9, 4639–4652, doi:10.5194/acp-9-4639-2009, 2009.
- Kirchner, U., Benter, T. H., and Schindler, R. N.: Experimental verification of gas phase bromine enrichment in reactions of HOBr with sea salt doped ice surfaces, *Ber. Bunsen Ges. Phys. Chem.*, 101, 975–977, 1997.
- König-Langlo, G., King, J. C., and Pettre, P.: Climatology of the three coastal Antarctic stations Dumont d'Urville, Neumayer, and Halley, *J. Geophys. Res.-Atmos.*, 103, 10935–10946, doi:10.1029/97jd00527, 1998.
- Kreher, K., Keys, J. G., Johnston, P. V., Platt, U., and Liu, X.: Ground-based measurements of OCIO and HCl in austral spring 1993 at Arrival Heights, Antarctica, *Geophys. Res. Lett.*, 23, 1545–1548, doi:10.1029/96gl01318, 1996.
- Kreher, K., Johnston, P. V., Wood, S. W., Nardi, B., and Platt, U.: Ground-based measurements of tropospheric and stratospheric BrO at Arrival Heights, Antarctica, *Geophys. Res. Lett.*, 24, 3021–3024, doi:10.1029/97gl02997, 1997.
- Landgraf, J. and Crutzen, P. J.: An Efficient Method for Online Calculations of Photolysis and Heating Rates, *J. Atmos. Sci.*, 55, 863–878, doi:10.1175/1520-0469(1998)055<0863:AEMFOC>2.0.CO;2, 1998.
- Leibrock, E. and Huey, L. G.: Ion chemistry for the detection of isoprene and other volatile organic compounds in ambient air, *Geophys. Res. Lett.*, 27, 1719–1722, 2000.
- Liao, J., Huey, L. G., Tanner, D. J., Brough, N., Brooks, S., Dibb, J. E., Stutz, J., Thomas, J. L., Lefer, B., Haman, C., and Gorham, K.: Observations of hydroxyl and peroxy radicals and the impact of BrO at Summit, Greenland in 2007 and 2008, *Atmos. Chem. Phys.*, 11, 8577–8591, doi:10.5194/acp-11-8577-2011, 2011a.
- Liao, J., Sihler, H., Huey, L. G., Neuman, J. A., Tanner, D. J., Friess, U., Platt, U., Flocke, F. M., Orlando, J. J., Shepson, P. B., Beine, H. J., Weinheimer, A. J., Sjostedt, S. J., Nowak, J. B., Knapp, D. J., Staebler, R. M., Zheng, W., Sander, R., Hall, S. R., and Ullmann, K.: A comparison of Arctic BrO measurements by chemical ionization mass spectrometry and long path-differential optical absorption spectroscopy, *J. Geophys. Res.-Atmos.*, 116,

- D00r02, doi:10.1029/2010jd014788, 2011b.
- Liao, J., Huey, L. G., Scheuer, E., Dibb, J. E., Stickel, R. E., Tanner, D. J., Neuman, J. A., Nowak, J. B., Choi, S., Wang, Y., Salawitch, R. J., Canty, T., Chance, K., Kurosu, T., Suleiman, R., Weinheimer, A. J., Shetter, R. E., Fried, A., Brune, W., Anderson, B., Zhang, X., Chen, G., Crawford, J., Hecobian, A., and Ingall, E. D.: Characterization of soluble bromide measurements and a case study of BrO observations during ARCTAS, *Atmos. Chem. Phys.*, 12, 1327–1338, doi:10.5194/acp-12-1327-2012, 2012a.
- Liao, J., Huey, L. G., Tanner, D. J., Flocke, F. M., Orlando, J. J., Neuman, J. A., Nowak, J. B., Weinheimer, A. J., Hall, S. R., Smith, J. N., Fried, A., Staebler, R. M., Wang, Y., Koo, J.-H., Cantrell, C. A., Weibring, P., Walega, J., Knapp, D. J., Shepson, P. B., and Stephens, C. R.: Observations of inorganic bromine (HOBr, BrO, and Br<sub>2</sub>) speciation at Barrow, Alaska, in spring 2009, *J. Geophys. Res.*, 117, D00R16, doi:10.1029/2011JD016641, 2012b.
- Neuman, J. A., Nowak, J. B., Huey, L. G., Burkholder, J. B., Dibb, J. E., Holloway, J. S., Liao, J., Peischl, J., Roberts, J. M., Ryerson, T. B., Scheuer, E., Stark, H., Stickel, R. E., Tanner, D. J., and Weinheimer, A.: Bromine measurements in ozone depleted air over the Arctic Ocean, *Atmos. Chem. Phys.*, 10, 6503–6514, doi:10.5194/acp-10-6503-2010, 2010.
- Oltmans, S. J.: Surface Ozone Measurements in Clean Air, *J. Geophys. Res.*, 86, 1174–1180, 1981.
- Piot, M. and von Glasow, R.: The potential importance of frost flowers, recycling on snow, and open leads for ozone depletion events, *Atmos. Chem. Phys.*, 8, 2437–2467, doi:10.5194/acp-8-2437-2008, 2008.
- Pöhler, D., Vogel, L., Friess, U., and Platt, U.: Observation of halogen species in the Amundsen Gulf, Arctic, by active long-path differential optical absorption spectroscopy, *P. Natl. Acad. Sci. USA*, 107, 6582–6587, doi:10.1073/pnas.0912231107, 2010.
- Rankin, A. M. and Wolff, E. W.: A year-long record of size-segregated aerosol composition at Halley, Antarctica, *J. Geophys. Res.-Atmos.*, 108, 4775, doi:10.1029/2003jd003993, 2003.
- Rankin, A. M., Wolff, E. W., and Martin, S.: Frost flowers: Implications for tropospheric chemistry and ice core interpretation, *J. Geophys. Res.-Atmos.*, 107, 4683, doi:10.1029/2002jd002492, 2002.
- Ridley, B. A., Walega, J. G., Dye, J. E., and Grahek, F. E.: Distributions of NO, NO<sub>x</sub>, NO<sub>y</sub>, and O<sub>3</sub> to 12 km altitude during the summer monsoon season over New Mexico, *J. Geophys. Res.*, 99, 25529–25534, doi:10.1029/94JD02210, 1994.
- Rolph, G. D.: Real-time Environmental Applications and Display sYstem (READY) Website (<http://ready.arl.noaa.gov>), NOAA Air Resources Laboratory, Silver Spring, MD, 2012.
- Roscoe, H. K. and Roscoe, J.: Polar tropospheric ozone depletion events observed in the International Geophysical Year of 1958, *Atmos. Chem. Phys.*, 6, 3303–3314, doi:10.5194/acp-6-3303-2006, 2006.
- Saiz-Lopez, A., Mahajan, A. S., Salmon, R. A., Bauguitte, S. J. B., Jones, A. E., Roscoe, H. K., and Plane, J. M. C.: Boundary layer halogens in coastal Antarctica, *Science*, 317, 348–351, doi:10.1126/science.1141408, 2007.
- Simpson, W. R., von Glasow, R., Riedel, K., Anderson, P., Ariya, P., Bottenheim, J., Burrows, J., Carpenter, L. J., Frieß, U., Goodsite, M. E., Heard, D., Hutterli, M., Jacobi, H.-W., Kaleschke, L., Neff, B., Plane, J., Platt, U., Richter, A., Roscoe, H., Sander, R., Shepson, P., Sodeau, J., Steffen, A., Wagner, T., and Wolff, E.: Halogens and their role in polar boundary-layer ozone depletion, *Atmos. Chem. Phys.*, 7, 4375–4418, doi:10.5194/acp-7-4375-2007, 2007.
- Sjostedt, S. J. and Abbatt, J. P. D.: Release of gas-phase halogens from sodium halide substrates: heterogeneous oxidation of frozen solutions and desiccated salts by hydroxyl radicals, *Environ. Res. Lett.*, 3, 045007, doi:10.1088/1748-9326/3/4/045007, 2008.
- Slusher, D. L., Pitteri, S. J., Haman, B. J., Tanner, D. J., and Huey, L. G.: A chemical ionization technique for measurement of pernitric acid in the upper troposphere and the polar boundary layer, *Geophys. Res. Lett.*, 28, 3875–3878, 2001.
- Slusher, D. L., Huey, L. G., Tanner, D. J., Flocke, F. M., and Roberts, J. M.: A thermal dissociation-chemical ionization mass spectrometry (td-cims) technique for the simultaneous measurement of peroxyacyl nitrates and dinitrogen pentoxide, *J. Geophys. Res.*, 109, D19315, doi:10.1029/2004JD004670, 2004.
- Spicer, C. W., Plastring, R. A., Foster, K. L., Finlayson-Pitts, B. J., Bottenheim, J. W., Grannas, A. M., and Shepson, P. B.: Molecular halogens before and during ozone depletion events in the Arctic at polar sunrise: concentrations and sources, *Atmos. Environ.*, 36, 2721–2731, 2002.
- Spreen, G., Kaleschke, L., and Heygster, G.: Sea ice remote sensing using AMSR-E 89-GHz channels, *J. Geophys. Res.-Oceans*, 113, C02s03, doi:10.1029/2005jc003384, 2008.
- Toyota, K., McConnell, J. C., Lupu, A., Neary, L., McLinden, C. A., Richter, A., Kwok, R., Semeniuk, K., Kaminski, J. W., Gong, S.-L., Jarosz, J., Chipperfield, M. P., and Sioris, C. E.: Analysis of reactive bromine production and ozone depletion in the Arctic boundary layer using 3-D simulations with GEM-AQ: inference from synoptic-scale patterns, *Atmos. Chem. Phys.*, 11, 3949–3979, doi:10.5194/acp-11-3949-2011, 2011.
- von Glasow, R., Sander, R., Bott, A., and Crutzen, P. J.: Modeling halogen chemistry in the marine boundary layer – 1. Cloud-free MBL, *J. Geophys. Res.-Atmos.*, 107, 4341, doi:10.1029/2001JD000942, 2002.
- Wesely, M. L.: Parameterization of surface resistances to gaseous dry deposition in regional-scale numerical models, *Atmos. Environ.*, 23, 1293–1304, 1989.
- Wessel, S., Aoki, S., Winkler, P., Weller, R., Herber, A., Gernandt, H., and Schrems, O.: Tropospheric ozone depletion in polar regions - A comparison of observations in the Arctic and Antarctic, *Tellus B*, 50, 34–50, 1998.
- Wilson, K. L. and Birks, J. W.: Mechanism and Elimination of a Water Vapour Interference in the Measurement of Ozone by UV Absorbance, *Environ. Sci. Technol.*, 40, 6361–6367, doi:10.1021/es052590c, 2006.
- Yang, X., Pyle, J. A., and Cox, R. A.: Sea salt aerosol production and bromine release: Role of snow on sea ice, *Geophys. Res. Lett.*, 35, L16815, doi:10.1029/2008GL034536, 2008.